



Simulations of a Thermostat Model I: Approach to Steady States

J. C. CHIPMAN, W. HOUTZ AND M. SHILLOR

Department of Mathematics and Statistics
Oakland University, Rochester, MI 48309, U.S.A.

(Received February 2000; accepted March 2000)

Abstract—Numerical simulations and analysis of the approach to steady states of a model for the dynamic behavior of an automotive thermostat-like system are presented. The model consists of a coupled system of three delay differential equations with hysteresis. This work is a continuation of our recent investigation of models for automotive thermostats in [1]. The main interest lies in the types of oscillations that such models can exhibit. This is done through the analysis of the steady states and the decay of the solutions to these states. © 2000 Elsevier Science Ltd. All rights reserved.

Keywords—Thermostat, Hysteresis, Delay, Oscillations, Numerical solutions.

1. INTRODUCTION

We continue the investigation of thermostat models, which has been conducted in [1–3]. These models are in the form of a coupled system of ordinary differential equations with delays and hysteresis. Our main interest in this paper lies in the steady states of the system and the way the solutions approach them.

The thermostats we investigate are thermomechanical devices situated in the car's cooling system which control the engine's operating temperature. They adjust the flow of the cooling fluid to the radiator so that an essentially optimal operating temperature range is maintained within the engine block. Since the cooling system is designed to handle extreme heat loads under which the engine may need to operate, only partial cooling capacity is required when driving under normal conditions. Indeed, if the cooling system were to operate at full capacity continuously, the engine would run too cold, well below its optimal operating temperature, leading to fuel inefficiency and unreasonable pollution. The thermostat senses the coolant temperature and allows a larger or smaller flow of coolant through the radiator, thereby keeping the coolant temperature almost constant. When the engine and the coolant are cold, the thermostat is closed and the flow to the radiator is fully diverted to a by-pass. Once the engine is running, the coolant temperature rises and the thermostat incrementally opens the flow path to the radiator. The flow splits between the part through the radiator and the part through the by-pass. Under heavy load conditions, the thermostat opens completely and then the full cooling capacity of the radiator is realized.

A dynamic model for automotive thermostats was derived recently in [1] where the full details can be found. In addition to the detailed modeling, numerical simulations were reported there showing the various types of solutions possible in such systems. Moreover, a thorough investigation of the conditions for oscillations was conducted in [1] using the statistical technique of response surface. The interest in the model, in addition to its applications in the automotive industry, stems from the fact that it includes *hysteresis*, since the way the thermostat opens when the temperature rises differs from the way it closes when the temperature decreases. Moreover, the cooling loop introduces delays into the system. The interplay between hysteresis and delay is of theoretical interest, and was partially analyzed in [2,3], where simpler models were investigated and numerically simulated.

In this paper, we derive the steady states, and study the approach to these states of solutions of a slightly simpler model than the one in [1].

The model is described in Section 2. It is taken from the model in [1] with two simplifications. The first consists of not including the heater and the second in not including the melting of the wax, which is the mechanism which at the heart of conventional thermostats. One may, therefore, consider the problem as modeling an electronic thermostat. In Section 3, we present analysis of the steady states of the system and distinguish between the case without hysteresis, in which there exists a unique steady state, and the model with hysteresis in which there exists a continuum of steady states. In Section 4, we show that the model without hysteresis has a global solution, and when the thermostat opening is fixed, the system approaches the steady state exponentially. In Section 5, we present a numerical algorithm for the problem, similar to the one in [1]. The numerical simulations are presented in Section 6. A brief summary of our results is given in Section 7, where we also indicate some remaining questions which may be of interest to address.

2. THE MODEL

In this section, we provide a short description of the model which we consider, taken from [1] with a number of simplifications. We refer the reader to [1] for a thorough explanation of the role of each system component and its modeling. We deal with a dynamic problem that describes the time behavior of a thermostat-like device which is situated in the car engine's cooling system. We consider the whole cooling loop which contains the thermostat, since we are interested in the (nonlinear) interactions among the loop components. For the sake of completeness, we present the full model of [1] in the Appendix.

The main difference between the system we consider here and the one in [1] is that we do not take into account the melting process of the wax which drives the automotive thermostat, indeed, the expansion of the wax upon melting provides the force necessary to open the valve. Here we just represent the dynamics of the thermostat by the hysteresis curve. One may consider such a system as describing a possible electronic thermostat.

A schematic diagram of the setting is depicted in Figure 1. Only the main elements in the cooling system are considered: radiator, engine, and bypass. For the sake of simplicity, we omit the passenger heater, which has been included in [1].

The basic assumptions underlying the model are that the energy source in the system is the engine; all the energy losses are in the radiator; the internal thermostat temperature differs from that of the coolant temperature. We describe the energy losses in the radiator and the thermal interaction between the thermostat and the coolant by Newton's Law of Cooling.

We denote the coolant temperature at the thermostat by $T = T(t)$, where t is the time variable, the temperature of the thermostat itself by $\theta(t)$, the radiator coolant temperature by $T_r = T_r(t)$, and the engine coolant temperature by $T_e = T_e(t)$. Since the thermostat is located in the engine, we set $T = T(t) = T_e(t)$. All the temperatures are in dimensionless units, scaled with respect to the ambient temperature.

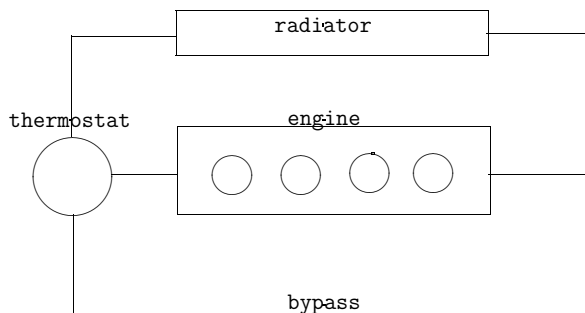


Figure 1. Schematic setting.

The thermo-mechanical information characterizing the thermostat is given by its hysteresis graph β , Figure 2, which consists of the two curves f_R, f_L , and the *hysteresis region* \mathcal{H} , which lies between them. The variable β describes the opening of the valve as a ‘function’ of the thermostat temperature θ . To be more precise, since β is a graph, we denote by $\omega = \omega(t)$ the fractional opening of the valve. When $\omega = 0$ it is closed, all the coolant flows via the bypass and heater loops, and there is no flow to the radiator. It is completely open when $\omega = 1$; this leads to maximum flow and cooling by the radiator. The thermostat is partially open when $0 < \omega < 1$. Then only the fraction ω of the fluid flows to the radiator, while the rest flows via the bypass. For the sake of simplicity, we depict f_R and f_L as straight lines in Figure 2. In applications both are monotone, smooth, and have a shape with one inflection point, and for further details see [1–3] and beginning of Section 3.1.

The way hysteresis affects the dynamic behavior is as follows. The curve f_R describes the way the valve opens. When the state of the thermostat $(\theta(t), \omega(t))$ is on the curve f_R and the temperature is rising, $\dot{\theta} > 0$, then the system continues to move along the curve f_R . We denote by T_R the smallest temperature for which $f_R = 1$. Next, the valve closes along f_L . If the temperature is decreasing, i.e., $\dot{\theta} < 0$, when $(\theta(t), \omega(t))$ is on f_L , the thermostat continues to move along the curve f_L . We denote by T_L the highest temperature for which $f_L = 0$. We note that $0 < T_L < T_R$.

Clearly, β depends on θ and on the sign of $\dot{\theta}$. It may happen however, that the system, while moving on f_R , reaches a time when $\dot{\theta}(t) = 0$ at a temperature $T_L < \theta(t) < T_R$, and afterwards the temperature decreases. To describe the system’s behavior in such a case, we assume the so-called ‘generalized play model’ (see, e.g., [4,5]) by which the system moves on the horizontal segment connecting the curves f_R and f_L , while the valve opening is $\omega = \text{const.}$ until it reaches the curve f_L , on which it continues to move down. We denote this behavior by the *hysteresis operator* H_β , and $\omega(t) = H_\beta(\theta(t), \dot{\theta}(t))$. We assume that \mathcal{H} is filled with a family of horizontal segments connecting the two curves, the ‘generalized play model.’

The model for the system evolution is constructed by following a small coolant element as it flows in the system, applying energy conservation at each component. For full details, we refer the reader to [1]. We make another simplification relative to [1] by assuming that there is only one delay in the system. It represents the time needed for a coolant element to travel from the engine to the radiator, from the radiator to the engine and from the engine to the engine via the bypass, and we denote in by τ .

The following system parameters are given positive (scaled) numbers: h_e -thermostat heat exchange coefficient; V_e -volume of coolant in the engine; V_r -volume of coolant in the radiator; q -engine heat generation rate; τ -system time delay; h_r -radiator heat exchange coefficient.

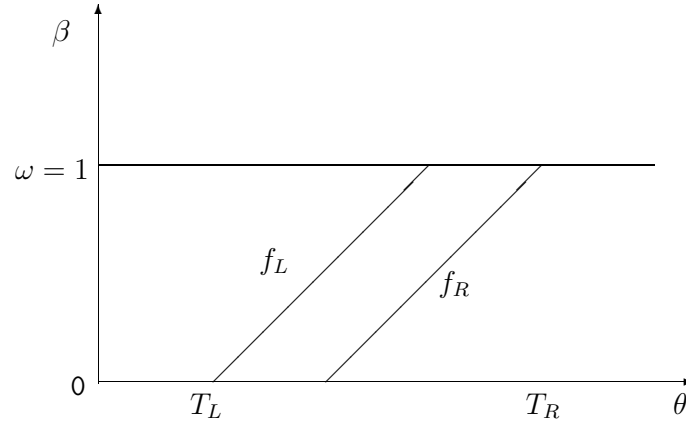


Figure 2. The hysteresis graph.

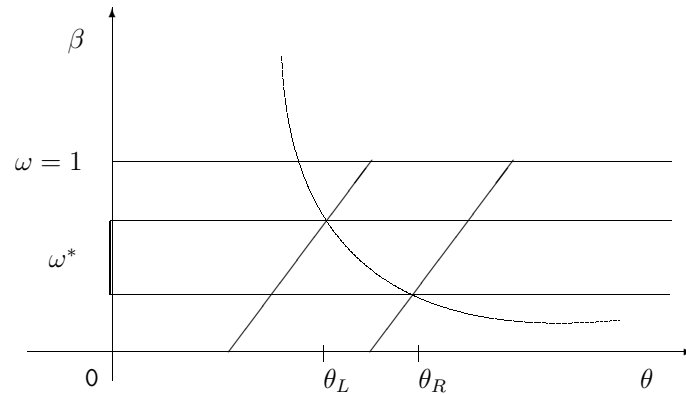


Figure 3. Multiple steady states.

The model (a modified version of [1]) is as follows. Find the functions $\{\theta, T_e, T_r, \omega\}$ such that

$$\frac{d\theta}{dt} = h_e(T_e(t) - \theta(t)), \quad (2.1)$$

$$\omega(t) = H_\beta(\theta(t)), \quad (2.2)$$

$$V_e \frac{dT_e}{dt} = q - (T_e(t) - T_e(t - \tau)) + \omega(t)(T_r(t - \tau) - T_e(t - \tau)), \quad (2.3)$$

$$V_r \frac{dT_r}{dt} = \omega(t)(T_e(t - \tau) - T_r(t)) - h_r T_r(t), \quad (2.4)$$

$$T_e(t) = T_{e0}(t), \quad T_r(t) = T_{r0}(t), \quad -\tau \leq t \leq 0, \quad (2.5)$$

$$\theta(0) = \theta_0, \quad \omega(0) = \omega_0. \quad (2.6)$$

Here, T_{e0} , T_{r0} , θ_0 , and ω_0 are the initial conditions: T_{e0} and T_{r0} are given functions defined on the time interval $-\tau \leq t \leq 0$. This is due to the existence of the delay in the system. The initial conditions for θ and ω are specified only at $t = 0$.

Detailed mathematical analysis of the model is not available yet. The problem is strongly nonlinear and includes hysteresis and a delay, therefore, questions of existence, uniqueness, and regularity of solutions need to be addressed. Also, sufficient conditions for appearance of self-induced oscillations are of considerable interest. Mathematical analysis of simplified models can be found in [2,3].

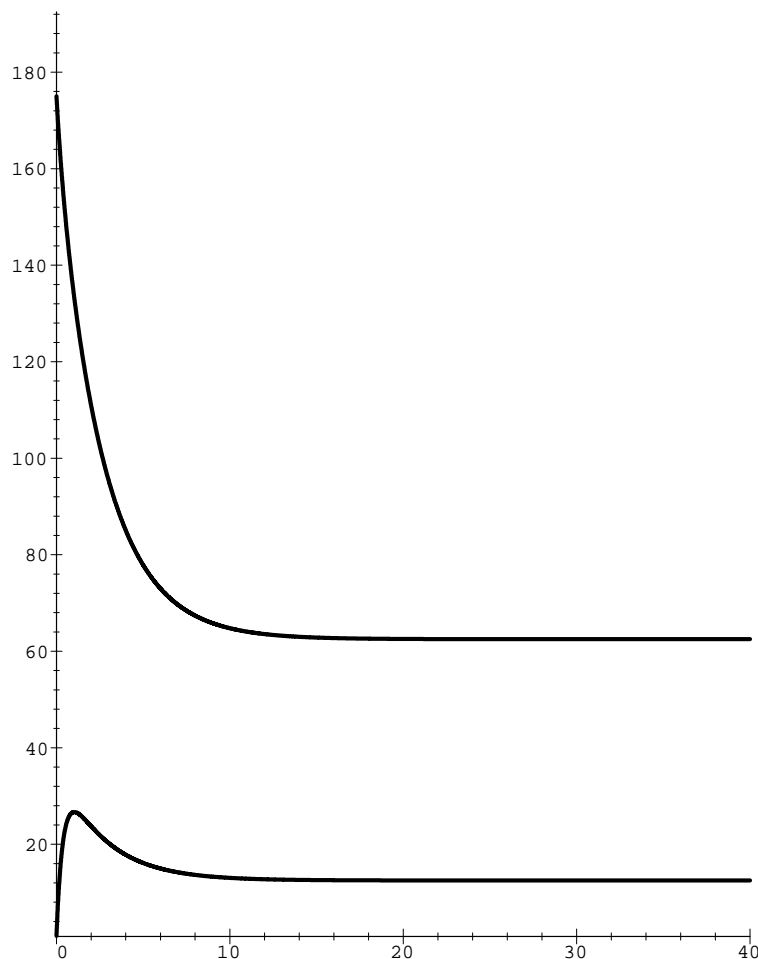


Figure 4. The graphs of T_e and T_r vs. time.

3. ANALYSIS OF STEADY STATES

In this section, we consider the steady states of system (2.1)–(2.6). In the following sections, we discuss the conditions for the solutions to converge to the steady states and numerically simulate them. In a steady state there is no dependence on the time, hence, we set $\tau = 0$ and suppress the references to t . After setting the derivatives equal to zero in (2.1), (2.3), and (2.4), the steady states of the system satisfy

$$\theta = T_e, \tag{3.1}$$

$$q = \omega(T_e - T_r), \tag{3.2}$$

$$\omega(T_e - T_r) = h_r T_r. \tag{3.3}$$

In addition, ω has to belong to the hysteresis graph.

Now, it follows from (3.2) and (3.3) that $q = h_r T_r$ or $T_r = q/h_r$. Substituting these values for T_e and T_r into (3.3) yields

$$\omega \left(\theta - \frac{q}{h_r} \right) = q.$$

Solving then for θ , we obtain

$$\theta = q \left(\frac{1}{\omega} + \frac{1}{h_r} \right).$$

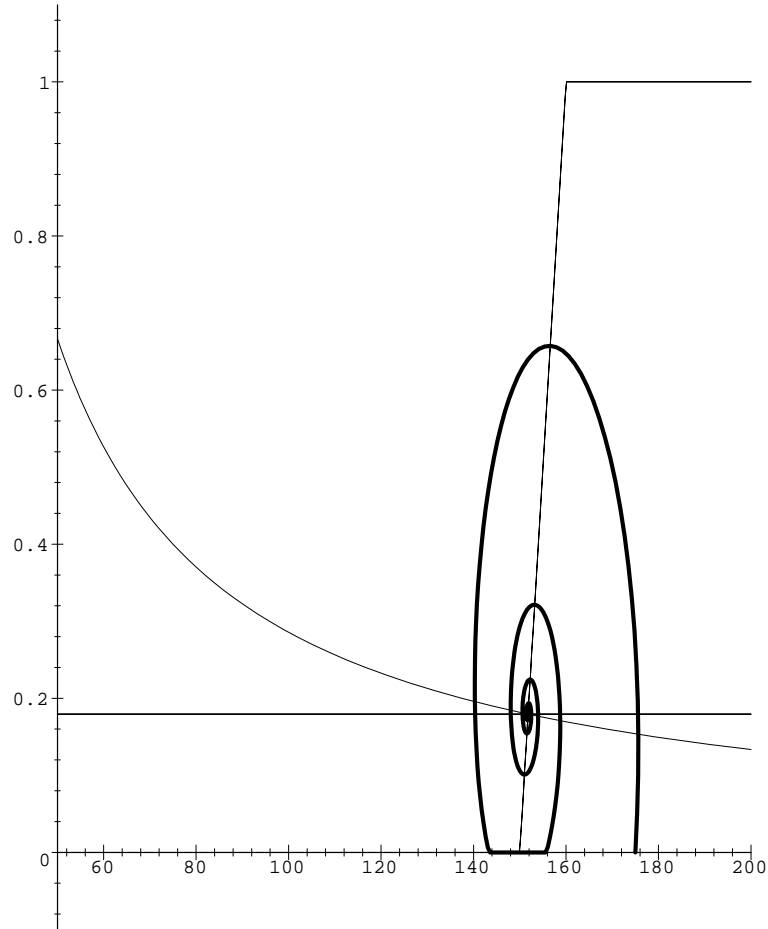
(a) $T_e - \omega$ plane.

Figure 5.

Combining these results, we obtain the following steady state conditions:

$$T_e = \theta, \quad (3.4)$$

$$T_r = \frac{q}{h_r}, \quad (3.5)$$

$$\theta = q \left(\frac{1}{\omega} + \frac{1}{h_r} \right). \quad (3.6)$$

An immediate conclusion is that if $q > 0$, then $\omega > 0$, which physically makes sense, since in the steady state the existence of a heat source ($0 < q$) implies the same rate of cooling in the radiator, $q = h_r T_r$, and therefore, a partially or fully open thermostat. Also, $T_e = \theta > T_r$ and $\theta > T_L$. Moreover, we note that if

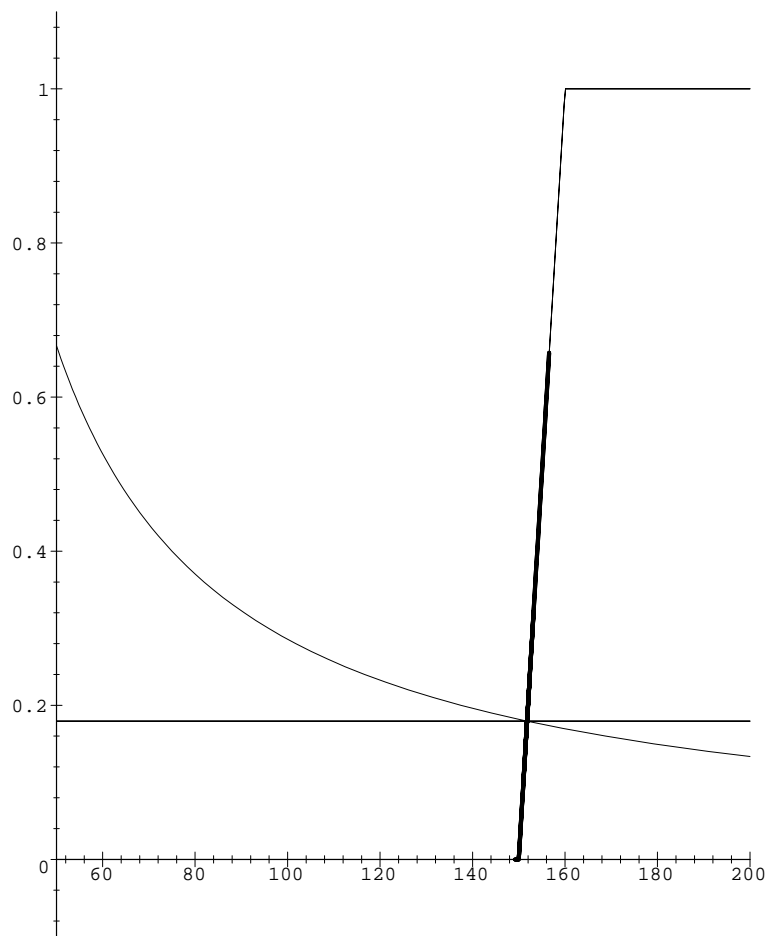
$$T_R \leq q \left(1 + \frac{1}{h_r} \right), \quad (3.7)$$

then $T_R \leq \theta = q(1 + 1/h_r)$ and $\omega = 1$. Otherwise, $\theta < T_R$ and $0 < \omega < 1$.

We note that when (3.7) does not hold, then

$$\frac{qh_r}{T_R h_r - 1} < \omega < 1.$$

We still need to determine θ and ω . To obtain a full characterization of the steady states, we consider the cases without and with hysteresis separately.



(b) $\theta - \omega$ plane; $q = 25$.

Figure 5. (cont.)

3.1. The Case Without Hysteresis

Assume first, that there is no hysteresis, i.e., that $f_L = f_R \equiv f$, and f is a smooth increasing function, satisfying $f(\theta) = 0$ for $\theta \leq T_L$, $f(\theta) = 1$ for $\theta \geq T_R$. Then, the steady state is obtained from the intersection of the curve $\omega = f(\theta)$ and the curve

$$\omega = \frac{qh_r}{\theta h_r - q}.$$

Therefore, the steady temperature θ is a root of the equation

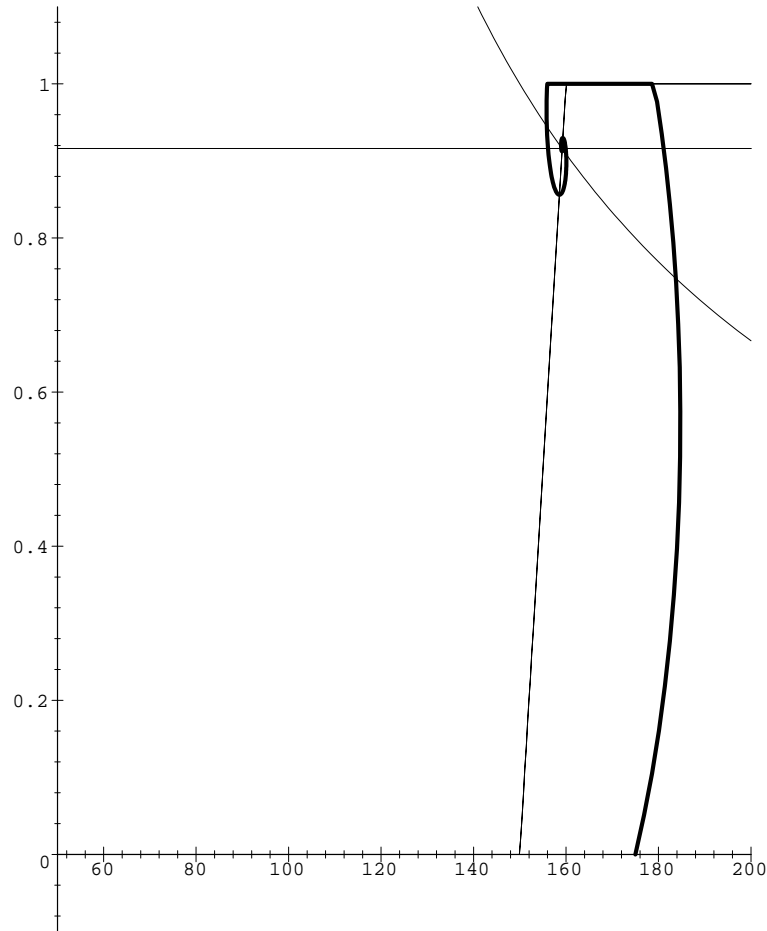
$$f(\theta) = \frac{qh_r}{\theta h_r - q}. \tag{3.8}$$

Now, the function $g(z) = (qh_r/zh_r - q)$ is strictly monotone decreasing, it approaches $+\infty$ as $z \rightarrow q/h_r$, and tends to 0 as $z \rightarrow \infty$, while f is nondecreasing, and thus, the solution θ is unique. When (3.7) holds then $\omega = 1$ and $\theta = q(1 + 1/h_r)$. On the other hand, if

$$q \left(1 + \frac{1}{h_r} \right) < T_R, \tag{3.9}$$

then $0 < \omega < 1$ and θ is the solution of (3.8) and satisfies $T_L < \theta < T_R$.

We summarize our findings in the case without hysteresis as follows.



(a) $T_e - \omega$ plane.

Figure 6.

PROPOSITION 3.1.

- (i) If $q(1 + 1/h_r) \geq T_R$, then $\omega = 1$ and $\theta = q(1 + 1/h_r)$.
- (ii) If $q(1 + 1/h_r) < T_R$, then $\omega = f(\theta)$ and θ is the unique root of (3.8).

3.2. The Case with Hysteresis

We next consider the problem with hysteresis. Now, there are two curves such that $f_R(\theta) < f_L(\theta)$ for $T_L < \theta < T_R$. A similar analysis as above shows that in this case, we have two values θ_L and θ_R obtained by solving the equations

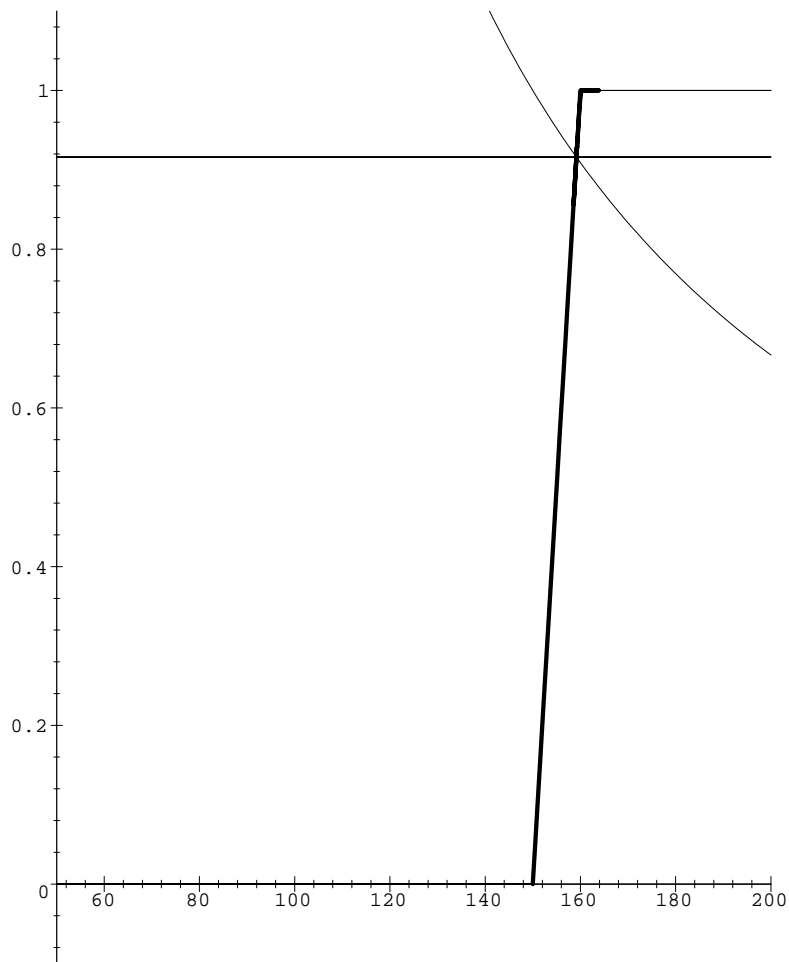
$$f_L(\theta_L) = \frac{qh_r}{\theta_L h_r - q}, \quad f_R(\theta_R) = \frac{qh_r}{\theta_R h_r - q}. \tag{3.10}$$

As can be seen in Figure 3, $T_L < \theta_L < \theta_R$, since g is strictly monotone decreasing and positive. Moreover, when (3.7) holds, we obtain

$$\omega = 1, \quad \theta = q \left(1 + \frac{1}{h_r} \right). \tag{3.11}$$

Here, θ is uniquely determined. When (3.9) holds the solution is not unique anymore, instead we have a set, actually two intervals, of steady solutions represented by

$$\theta_L \leq \theta^* \leq \theta_R, \quad \omega^* = \frac{qh_r}{\theta^* h_r - q}. \tag{3.12}$$



(b) $\theta - \omega$ plane; $q = 100$.

Figure 6. (cont.)

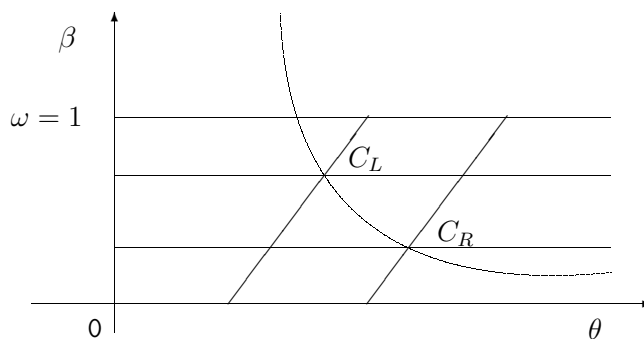


Figure 7. The $\theta - \omega$ plane with hysteresis and g .

Thus, for each θ^* in the interval $[\theta_L, \theta_R]$ we have the corresponding ω^* , as depicted by the thick line in Figure 3. If we solve system (2.1)–(2.6) with the initial conditions $T_{e0} = \theta^*, T_{r0} = q/h_r, \theta_0 = \theta^*, \omega_0 = \omega^*$, it will remain in this state.

Now, the interesting question is which of these steady states are obtainable in the limit $t \rightarrow \infty$ starting from initial conditions which are not a steady state. The mathematical analysis of this topic lies in the future. However, we investigate this problem numerically in Section 6.2, and

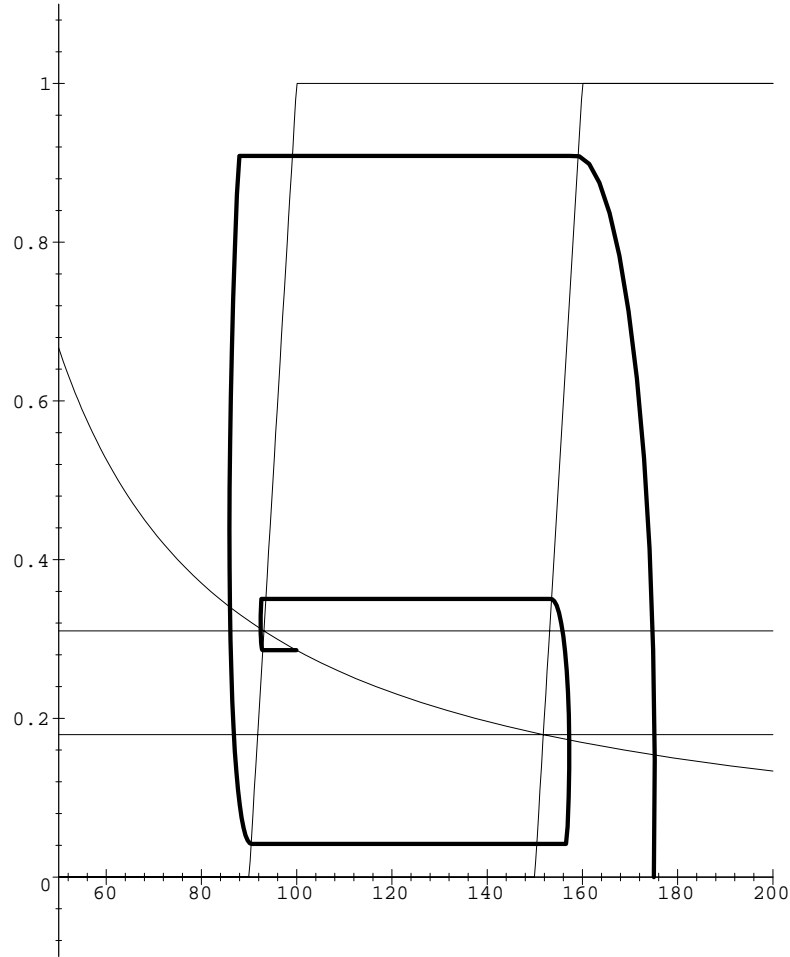
(a) $T_e - \omega$ plane.

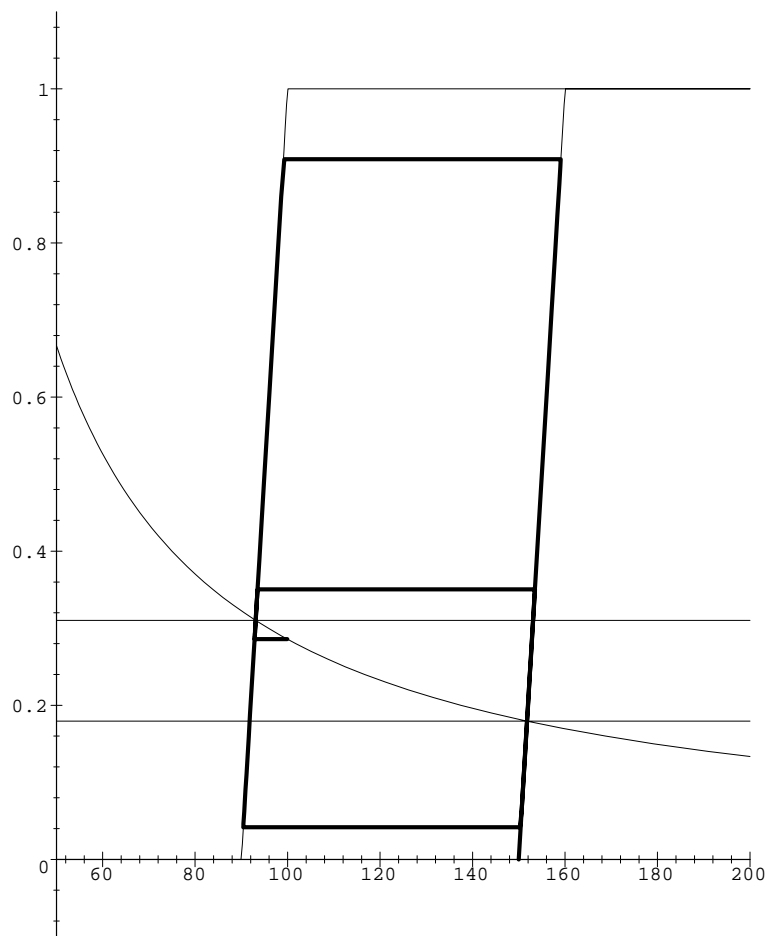
Figure 8.

based on these simulations we conjecture that *by choosing appropriately the initial conditions T_{e0} , T_{r0} , and θ_0 together with ω_0 , such that $\omega_0 = H_\beta(\theta_0)$, but not as steady conditions, each of the steady states (3.12) can be reached asymptotically.*

Actually, if we relax the condition $\omega_0 = H_\beta(\theta_0)$, and allow any $\omega_0 \in (0, 1)$, then the numerical simulations indicate that other steady states are possible too. However, we do not pursue this topic here any further, since it lies outside of our physical interpretation of the model.

4. THE PROBLEM WITHOUT HYSTERESIS

We investigate a simplified system which results when we disregard the delay ($\tau = 0$) and the hysteresis. Therefore, we assume that $f_L = f_R = f$, where f is a smooth increasing function satisfying $f(\theta) = 0$ for $\theta \leq T_L$, $f(\theta) = 1$ for $\theta \geq T_R$, and $f' > 0$ for $\theta_L < \theta < \theta_R$. The steady state problem for this system is given in Section 3.1. For the sake of simplicity, below we set $V_e = V_r = 1$. However, now ω is not a dependent variable, it is determined from f , indeed, $\omega(t) = f(\theta(t))$, so we rewrite the system by replacing ω with $f(\theta)$.



(b) $\theta - \omega$ plane.

Figure 8. (cont.)

The problem without hysteresis and without delay is as follows. Find the functions $\{\theta, T_e, T_r\}$ such that

$$\frac{d\theta}{dt} = h_e(T_e(t) - \theta(t)), \tag{4.1}$$

$$\frac{dT_e}{dt} = q - f(\theta(t))(T_e(t) - T_r(t)), \tag{4.2}$$

$$\frac{dT_r}{dt} = f(\theta(t))(T_e(t) - T_r(t)) - h_r T_r(t), \tag{4.3}$$

$$T_e(0) = T_{e0}, \quad T_r(0) = T_{r0}, \quad \theta(0) = \theta_0. \tag{4.4}$$

Here, we used the notation as in (2.1)–(2.5), except that $\tau = 0$.

Since all the data functions are globally Lipschitz continuous, we obtain from the theory of ODEs that problems (4.1)–(4.4) have a unique local solution.

Next, we show that the solution $\{\theta, T_e, T_r\}$ is global in time, and is bounded.

PROPOSITION 4.1. *Assume that the initial data satisfies*

$$T_{e0} \leq m_0, \quad T_{r0} \leq m_0, \quad \theta_0 \leq m_0.$$

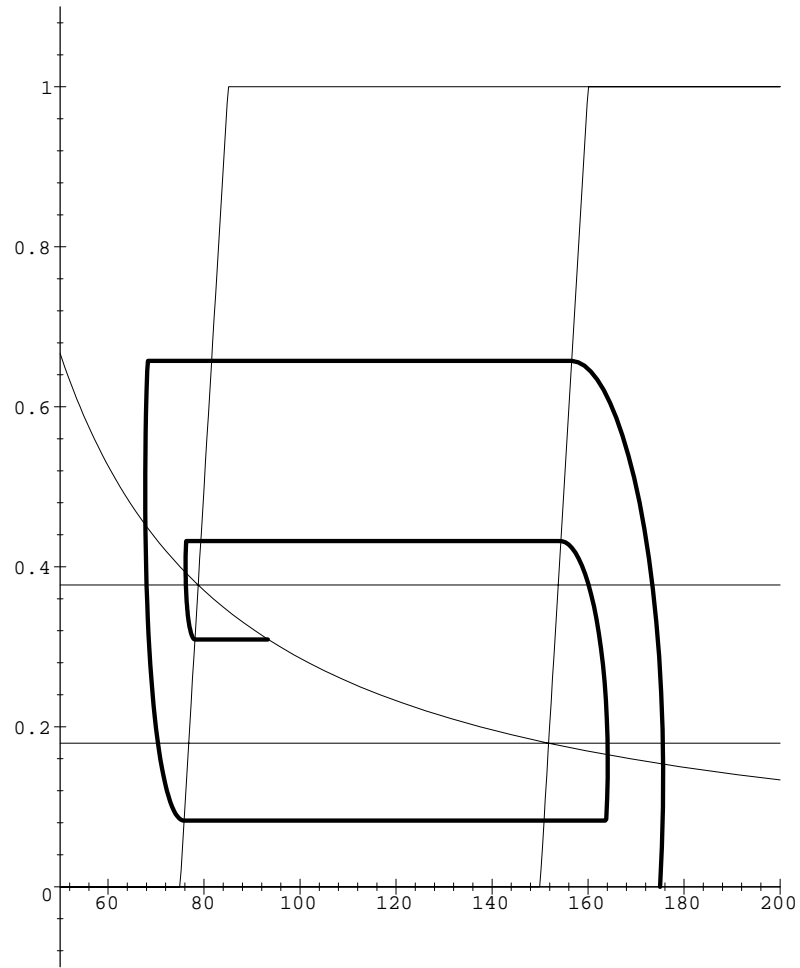
(a) $T_e - \omega$ plane.

Figure 9.

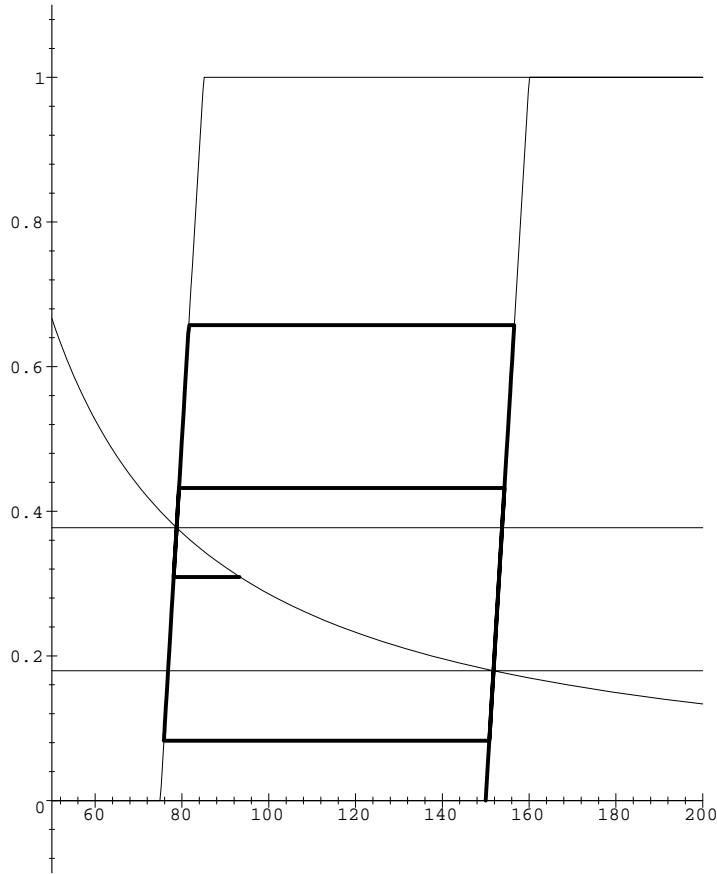
Then, the solution $\{\theta, T_e, T_r\}$ of (4.1)–(4.4) exists on $[0, +\infty)$, and satisfies

$$\theta(t) \leq M, \quad (4.5)$$

$$T_e(t) \leq M, \quad (4.6)$$

$$T_r(t) \leq M, \quad (4.7)$$

for all $0 \leq t$, where M is a positive constant, which depends only on T_R , m_0 , q , and h_r .



(b) $\theta - \omega$ plane.

Figure 9. (cont.)

PROOF. Once we establish (4.5)–(4.7), we may conclude that the solution exists for all time.

We choose $\max \{T_R, m_0, q(1 + 1/h_r)\} < M$ and let t_1 be the first time when $T_e(t_1) = M$ and $0 < T'_e(t_1)$. If such a time does not exist, then T_e satisfies (4.6) and the rest of the proof is straightforward. Also, it follows from (4.1) that if M is sufficiently large, then $T_R \leq \theta(t_1)$, since otherwise, $\theta'(t_1) > 0$ and large, and thus, we may assume that $f(\theta(t_1)) = 1$. Then, (4.2) implies that $0 < q - M + T_r(t_1)$, and so $M - q < T_r(t_1)$ and then (4.3) yields

$$T'_r(t_1) = q - h_r T_r < q - h_r(M - q) < (1 + h_r)q - h_r M < 0.$$

Hence, T_r is decreasing at t_1 . So let $t_2 < t_1$ be the nearest maximum of T_r preceding t_1 , i.e., $T'_r(t_2) = 0$. If such t_2 cannot be found, then $T_r \leq m_0$ and the rest of the proof is straightforward. Then (4.3) implies, assuming $f(\theta(t_2)) = 1$, that $0 = T_e(t_2) - T_r(t_2) - h_r T_r(t_2)$ or $T_e(t_2) = (1 + h_r)T_r(t_2)$, and then (4.2) yields

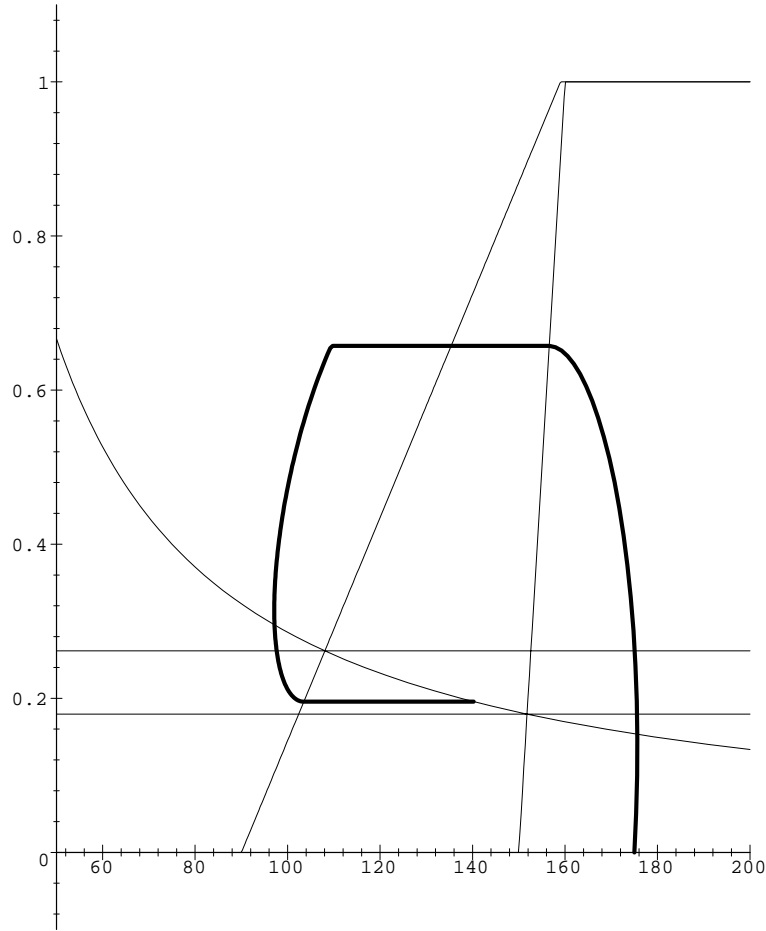
$$T'_e(t_2) = q - h_r T_r(t_2) < q - h_r(M - q) = (1 + h_r)q - h_r M < 0.$$

Hence, T_e is decreasing at $t = t_2$, and moreover,

$$T_e(t_2) = (1 + h_r)T_r > (1 + h_r)(M - q) > M + h_r M - (1 + h_r)q > M.$$

This contradicts the choice of t_1 , and therefore, T_e is bounded by M , for a sufficiently large M . Then it follows from (4.3) that $T_r < M$. Otherwise, let t_3 be the first time such that $T_r(t_3) = M$. Then

$$T'_r(t_3) = T_e(t_3) - (1 + h_r)T_r(t_3) \leq M - (1 + h_r)M \leq -h_r M < 0,$$



(a) $T_e - \omega$ plane.

Figure 10.

but then it means that $T_r(t) \geq M$ for $t \leq t_3$, a contradiction to the choice of t_3 . We conclude that (4.7) holds. Finally, since T_e is bounded it follows from (4.1) that θ is bounded by M as well. Indeed, let t_4 be the first time when $\theta(t_4) = M + \epsilon$ for a small positive ϵ . Then it follows from (4.1) that $\theta'(t_4) < -\epsilon h$, a contradiction.

The proof of the convergence of $\{\theta, T_e, T_r\}$ to the steady solution of Section 3.1 remains open. However, in the case when $\omega = \text{const.}$, we can show it as follows.

First, we note that in this case the problem reduces to solving the system

$$\frac{dT_e}{dt} = q - \omega(T_e(t) - T_r(t)), \tag{4.8}$$

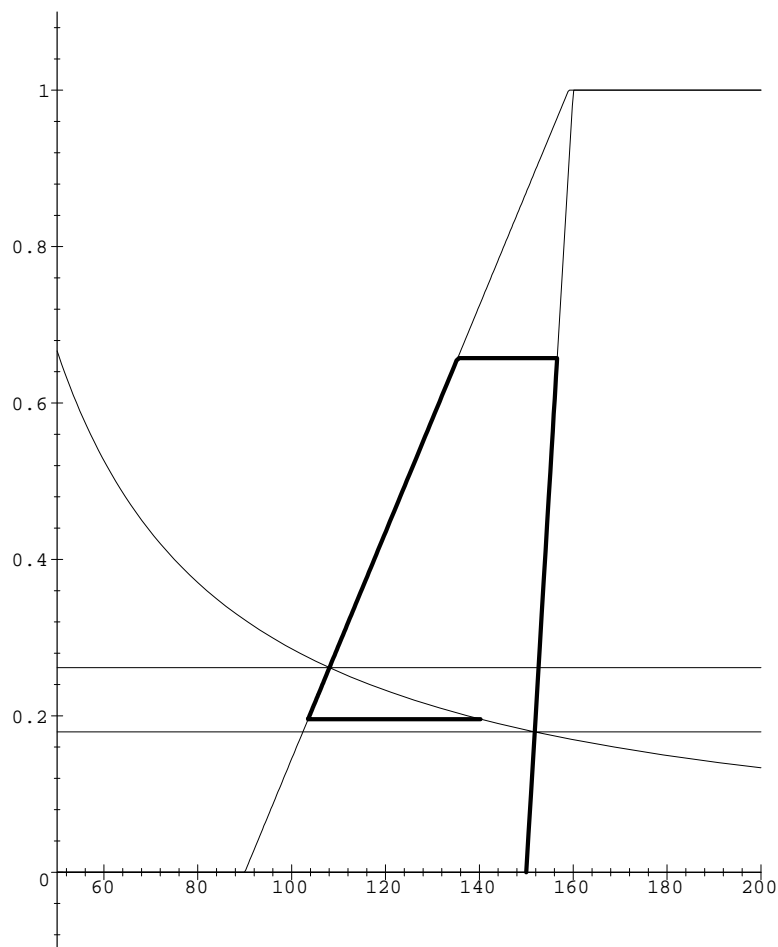
$$\frac{dT_r}{dt} = \omega(T_e(t) - T_r(t)) - h_r T_r(t), \tag{4.9}$$

$$T_e(0) = T_{e0}, \quad T_r(0) = T_{r0}. \tag{4.10}$$

Once T_e and T_r have been found, θ is obtained by solving (4.1).

We note that when $\omega = 0$ the right-hand side of (4.9) vanishes, and so $T_r(t) = T_{r0}$, and it follows from (4.8) that $T_e(t) = T_{e0} + qt$, and therefore, $T_e(t) \rightarrow +\infty$ as $t \rightarrow +\infty$. This is not surprising, since in this case, there is no cooling and the constant input of energy at rate q causes the temperature to grow without any bound.

We assume in the sequel that $0 < \omega = \text{const.}$ Let \bar{T}_e , \bar{T}_r , and $\bar{\theta}$ denote the steady state solution



(b) $\theta - \omega$ plane.

Figure 10. (cont.)

of (4.8)–(4.10), found in Section 3, namely,

$$\bar{T}_e = q \left(\frac{1}{\omega} + \frac{1}{h_r} \right), \quad \bar{T}_r = \frac{q}{h_r}.$$

We define two new dependent variables φ and ψ as follows,

$$\varphi(t) = T_e(t) - \bar{T}_e, \quad \psi(t) = T_r(t) - \bar{T}_r. \tag{4.11}$$

Then, φ and ψ satisfy the system

$$\frac{d\varphi}{dt} = -\omega(\varphi - \psi), \tag{4.12}$$

$$\frac{d\psi}{dt} = \omega(\varphi - \psi) - h_r\psi, \tag{4.13}$$

$$\varphi(0) = T_{e0} - \bar{T}_e, \quad \psi(0) = T_{r0} - \bar{T}_r. \tag{4.14}$$

We show that $\varphi, \psi \rightarrow 0$ as $t \rightarrow \infty$, and therefore, $T_e \rightarrow \bar{T}_e$ and $T_r \rightarrow \bar{T}_r$ as $t \rightarrow \infty$.
Let $V = V(t)$ be the function

$$V = \varphi^2 + \psi^2.$$

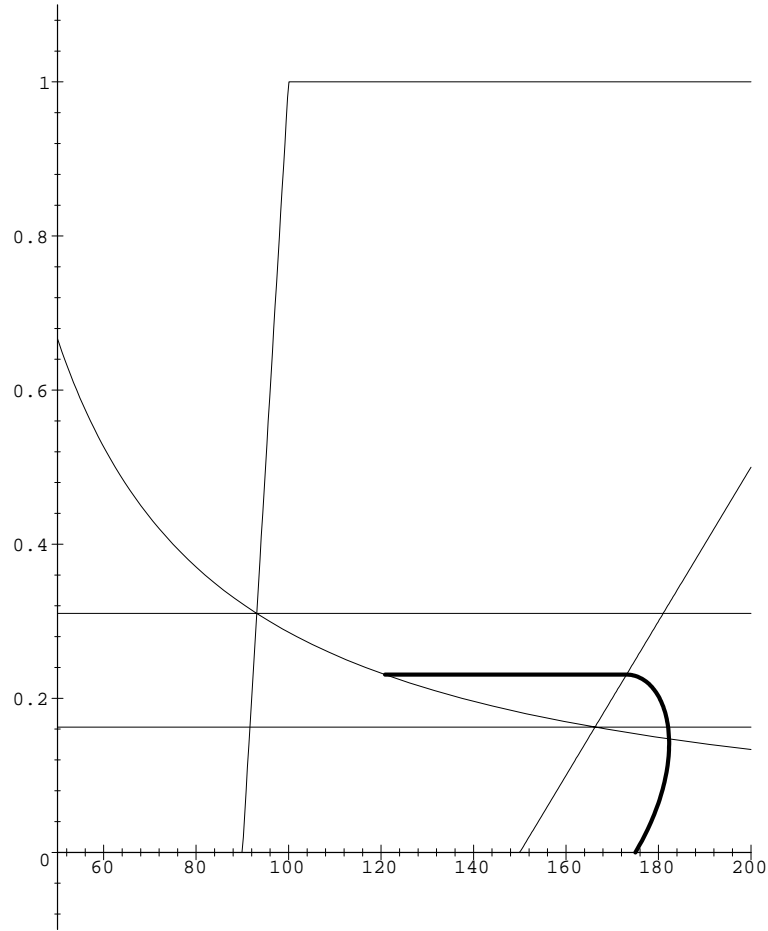
(a) $T_e - \omega$ plane.

Figure 11.

Then, we may use V as a Liapunov function for system (4.12)–(4.14). Indeed, using (4.12) and (4.13), we obtain

$$\frac{dV}{dt} = -2\omega(\varphi - \psi)^2 - 2h_r\psi^2 \leq 0.$$

Thus, the Liapunov function V satisfies: $0 \leq V$, it is bounded, and therefore, both φ and ψ are bounded, and $V' \leq 0$. We conclude that the trajectories of the system are bounded. Moreover, if either φ or ψ do not approach zero, then V' is strictly negative and so V will eventually become negative, which is impossible.

Another way to see it is the following.

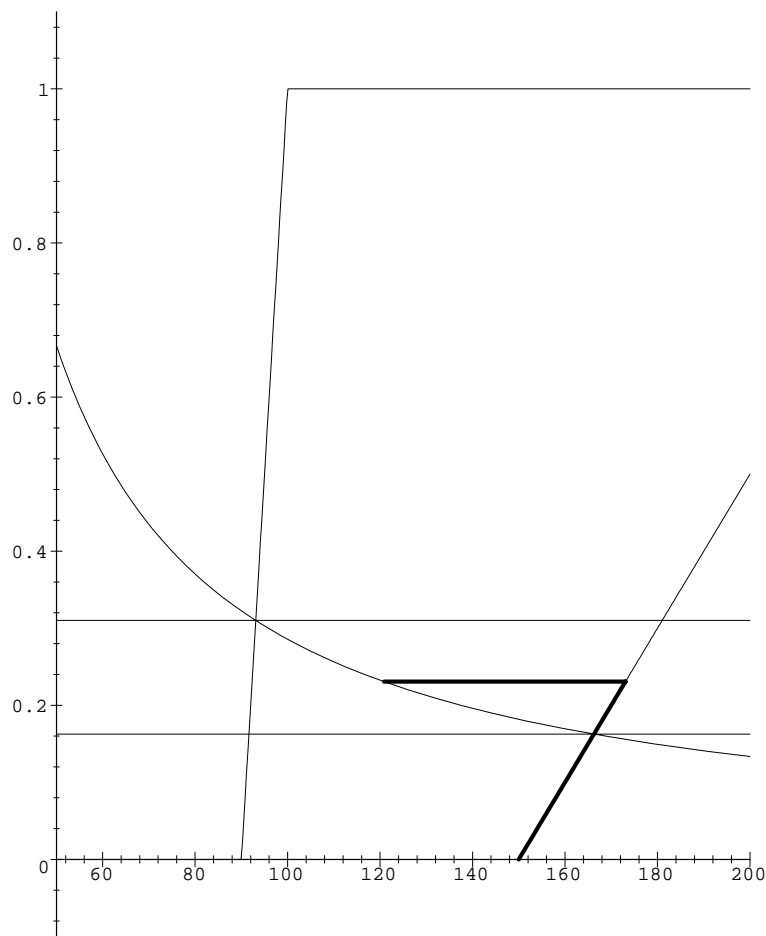
PROPOSITION 4.2. *The unique steady solution $(0, 0)$ of system (4.12)–(4.14) is asymptotically stable, or attracting.*

PROOF. We write the system as

$$\begin{pmatrix} \varphi \\ \psi \end{pmatrix}' = \omega \begin{pmatrix} -1 & 1 \\ 1 & -(1 + h_*) \end{pmatrix} \begin{pmatrix} \varphi \\ \psi \end{pmatrix},$$

where $h_* = h_r/\omega$. Now, the matrix A ,

$$A = \begin{pmatrix} -1 & 1 \\ 1 & -(1 + h_*) \end{pmatrix},$$



(b) $\theta - \omega$ plane.

Figure 11. (cont.)

is negative definite, with eigenvalues

$$\lambda_{1,2} = -\left(1 + \frac{1}{2}h_*\right) \pm \sqrt{1 + \frac{1}{4}h_*^2},$$

which are both negative, indeed, $\lambda_{1,2} < -h/(2 + h) = -h_r/(2\omega + h_r)$. Therefore, $(0, 0)$ is stable and attracting, and by standard linear stability theory for ODEs the system approaches the unique steady solution $(0, 0)$ exponentially.

This result indicates that the Liapunov function decays exponentially to zero too.

5. NUMERICAL ALGORITHM

We present the algorithm used to obtain numerical solutions of model (2.1)–(2.6), and the the simplified version without delay or hysteresis, (4.1)–(4.4). The results of the numerical simulations will be given in the following section.

We employ the explicit Euler method to solve the system of ordinary differential equations (2.1)–(2.6). Let Δt be the discretization time step and $N = T/\Delta t$ be the number of time steps. We denote by T_e^j , θ^j , T_r^j , and ω^j the values of the functions at time $t = j\Delta t$, i.e.,

$$T_e^j = T_e(j\Delta t), \quad \theta^j = \theta(j\Delta t), \quad T_r^j = T_r(j\Delta t), \quad \text{and} \quad \omega^j = \omega(j\Delta t),$$

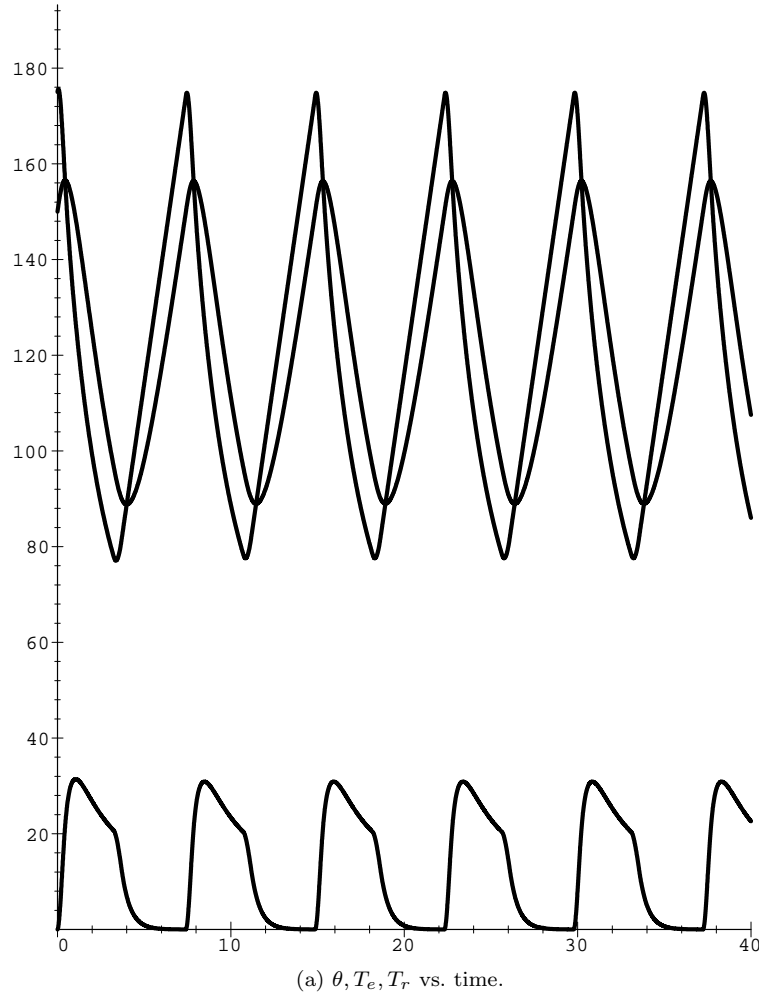


Figure 12.

for $0 \leq j \leq N$. These denote the finite differences approximations to the engine, thermostat, and radiator temperatures and the thermostat opening at time $j\Delta t$, respectively. To deal with the delay let d be the closest integer to $\tau/\Delta t$.

Since we deal with a system with delay, we initialize the variables by setting

$$T_e^j = T_{e0}(j\Delta t), \quad T_r^j = T_{r0}(j\Delta t), \quad \text{for } -d \leq j \leq 0,$$

together with

$$\theta^0 = \theta_0, \quad \omega^0 = \omega_0.$$

We note that the values of ω^j for $-d + 1 \leq j \leq 0$ are determined from those of θ^j and the hysteresis operator H_β .

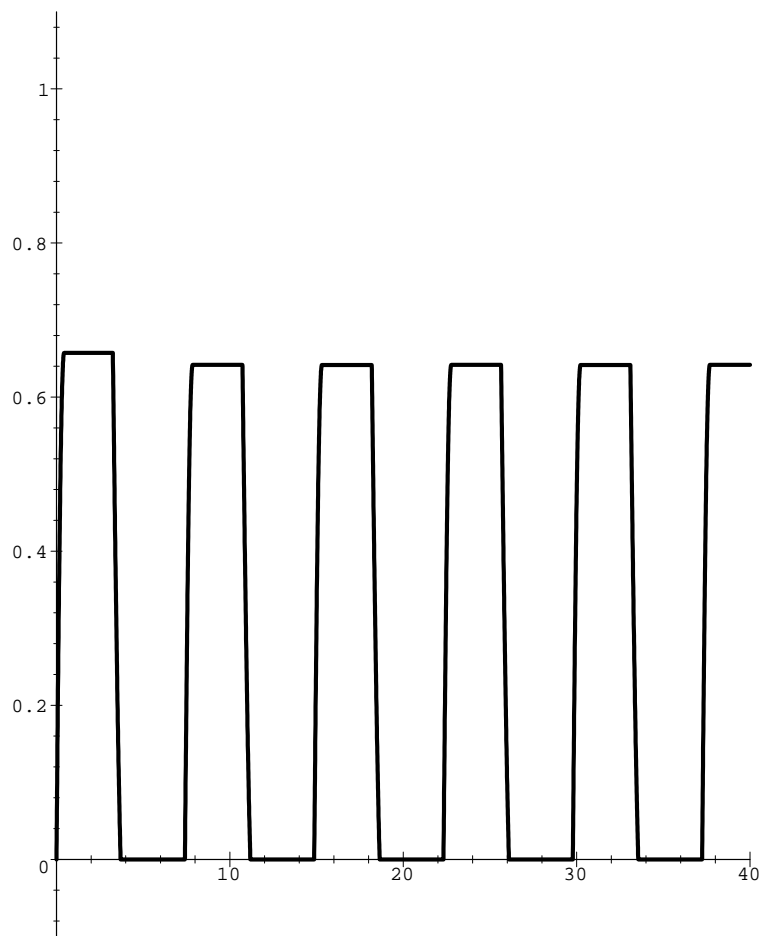
For the sake of simplicity, as in Section 4, we assume that $V_r = V_e = 1$, so that the system parameters are q , h_r , and h_e .

Now, the algorithm proceeds in (time) steps. Assume that at the step j all the function values $\{\theta^k, T_e^k, T_r^k, \omega^k\}$ have been determined for $0 \leq k \leq j$. Then the values $\{\theta^{j+1}, T_e^{j+1}, T_r^{j+1}, \omega^{j+1}\}$ are determined as follows.

First, the thermostat temperature θ^{j+1} , is computed from (2.1) by

$$\theta^{j+1} = \theta^j + h_e \Delta t (T_e^j - \theta^j). \quad (5.1)$$

Then, we compute the new opening ω^{j+1} from the hysteresis curves and the play model assumption as follows: if $\omega^j = f_R(\theta^j)$ and ω is increasing, then the opening follows f_R , when $\omega^j = f_L(\theta^j)$



(b) ω vs. time, intrinsic oscillations.

Figure 12. (cont.)

and θ is decreasing the opening follows the curve f_L , otherwise the opening is constant, at the same value as in the previous time step. In terms of coding, we use the following.

```

if ( $\theta[i] = \theta[i - 1]$ ) then
     $\omega[i] := \omega[i - 1]$ 
fi;
if ( $\theta[i] > \theta[i - 1]$ ) then
    if ( $f_R(\theta[i]) \geq \omega[i - 1]$ ) then
         $\omega[i] := f_R(\theta[i])$ 
    else
         $\omega[i] := \omega[i - 1]$ 
    fi
fi;
if ( $\theta[i] < \theta[i - 1]$ ) then
    if ( $f_L(\theta[i]) \leq \omega[i - 1]$ ) then
         $\omega[i] := f_L(\theta[i])$ 
    else
         $\omega[i] := \omega[i - 1]$ 
    fi
fi.
    
```

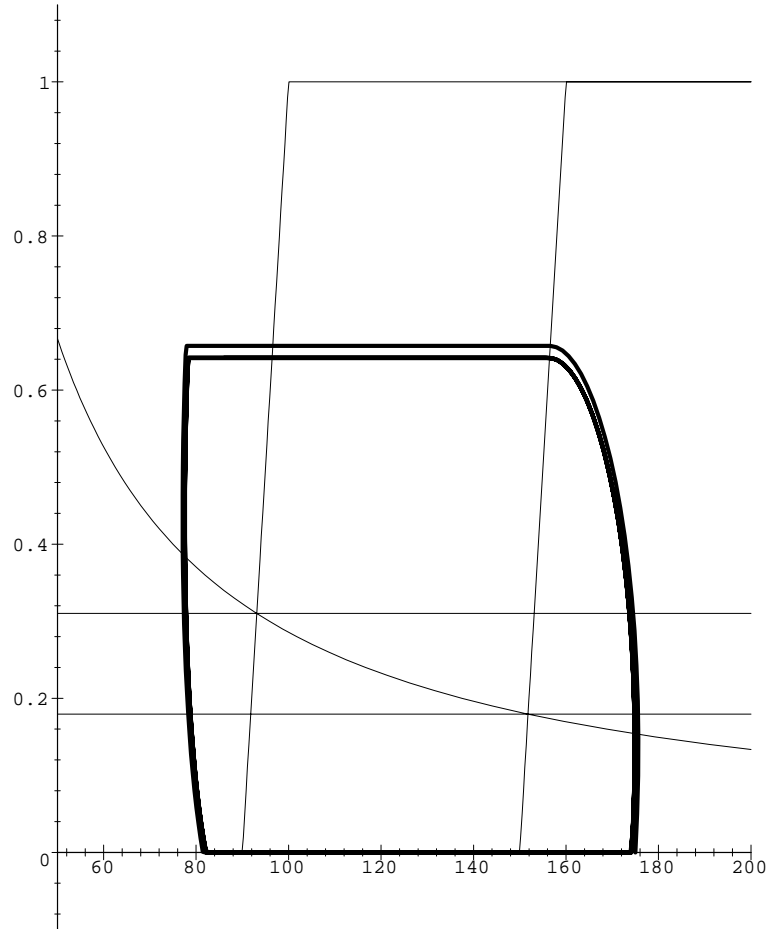
(c) $T_e - \omega$ plane.

Figure 12. (cont.)

Next, the engine temperature is computed from (2.3) using the formula

$$T_e^{j+1} = T_e^j + \Delta t (q - T_e^j + w^{j+1} T_r^{j-d} + (1 - w^{j+1}) T_e^{j-d}). \quad (5.2)$$

Finally, we compute the radiator temperature from (2.4) by

$$T_r^{j+1} = T_r^j + \Delta t (-h_r T_r^j + w^{j+1} (T_e^{j-d} - T_r^j)). \quad (5.3)$$

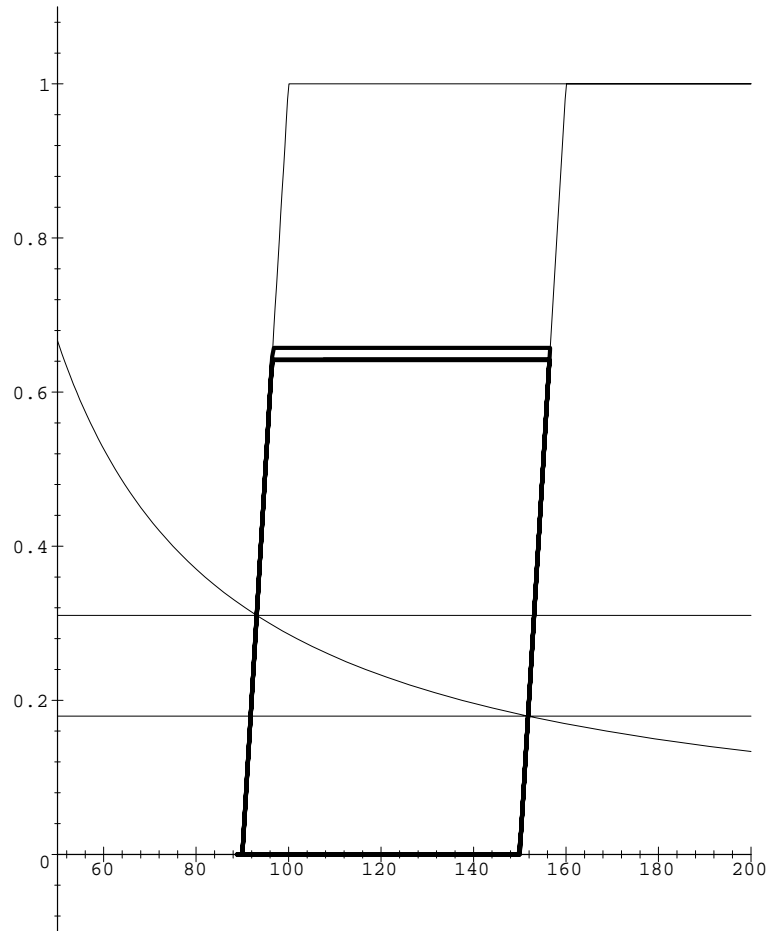
We note that both T_e^{j+1} and T_r^{j+1} are computed with ω^{j+1} . And the process repeats itself for $j + 2$.

The numerical simulations are described in the next section.

6. SIMULATIONS OF THE APPROACH TO STEADY STATES

In this section, we investigate numerically the approach of the solutions of problems (2.1)–(2.6) to their steady states, given in Section 3.2, and those of system (4.1)–(4.4) given in Section 3.1. We use the algorithm described in the previous section.

We begin the investigation with solutions of system (4.8)–(4.10), where $\omega = \text{const.} \in (0, 1)$. Then we investigate system (4.1)–(4.4), where $\omega = f(\theta)$. Next is system (2.1)–(2.6), with hysteresis, but without delay. Finally, we briefly consider system (2.1)–(2.6) with delay $0 < \tau$.



(d) $\theta - \omega$ plane.

Figure 12. (cont.)

6.1. The Case of Constant ω and No Delay

We now present the results for system (4.8)–(4.10) together with (4.1). It follows from Proposition 4.2 that all the solutions decay exponentially to the unique steady state. This behavior of T_e and T_r as a function of time is depicted in Figure 4. We set $T_{e0} = 175$, $T_{r0} = 1$, $\theta_0 = 150$, and $\omega_0 = 0.5$, and the system constants were $q = 25$, $h_r = 2.0$, $h_e = 1$, the time steps were $\Delta t = 0.005$ and final time $T = 40$.

6.2. The Case Without Hysteresis or Delay

Next, we describe simulations of the problem with no delay or hysteresis, but with $\omega = f(\theta)$, system (4.1)–(4.4). We set the system constants as $h_r = 2.0$, $h_e = 1$, $T_L = 150$, $T_R = 160$, the time step was $\Delta t = 0.005$, and the number of steps was 8000, i.e., $T = 40$. The initial conditions were $T_{e0} = 175$, $T_{r0} = 0$, $\theta_0 = 150$, and $\omega_0 = 0$. In Figure 5, $q = 25$ and in Figure 6, $q = 100$, and in both figures, we present the evolution of the system in (a) the $T_e - \omega$ plane, and (b) in the $\theta - \omega$ plane. We see that in both simulations the solutions oscillate and converge to the steady solutions, respectively.

6.3. The Case with Hysteresis and Without Delay

We now describe simulations of system (2.1)–(2.6), but without the delay ($\tau = 0$). For the sake of simplicity we, again, set $V_e = V_r = 1$.

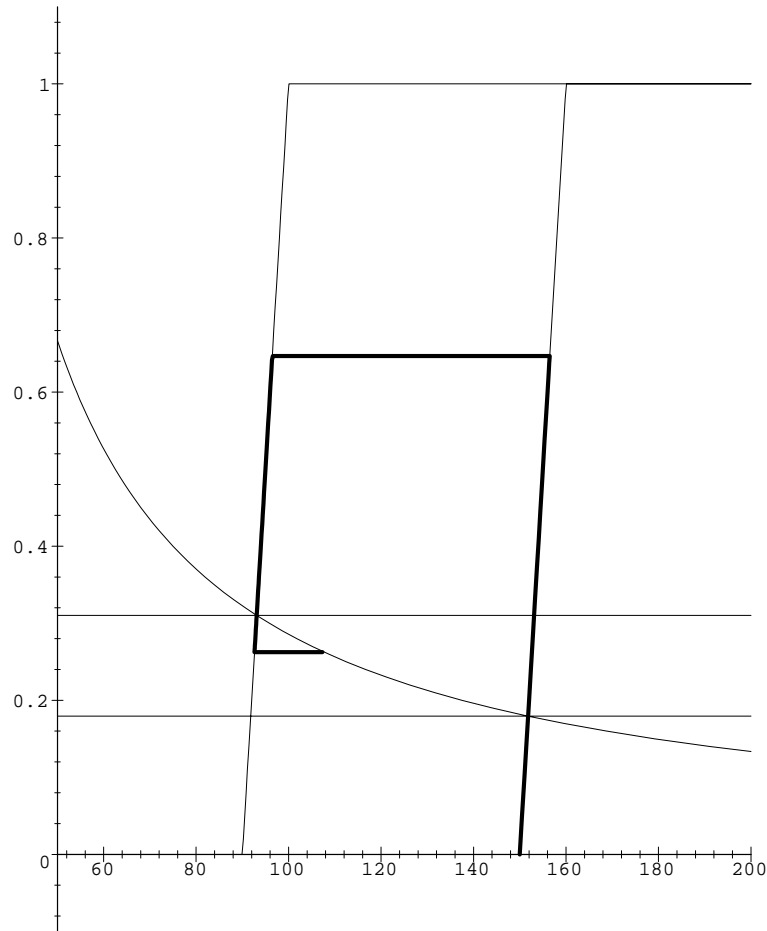
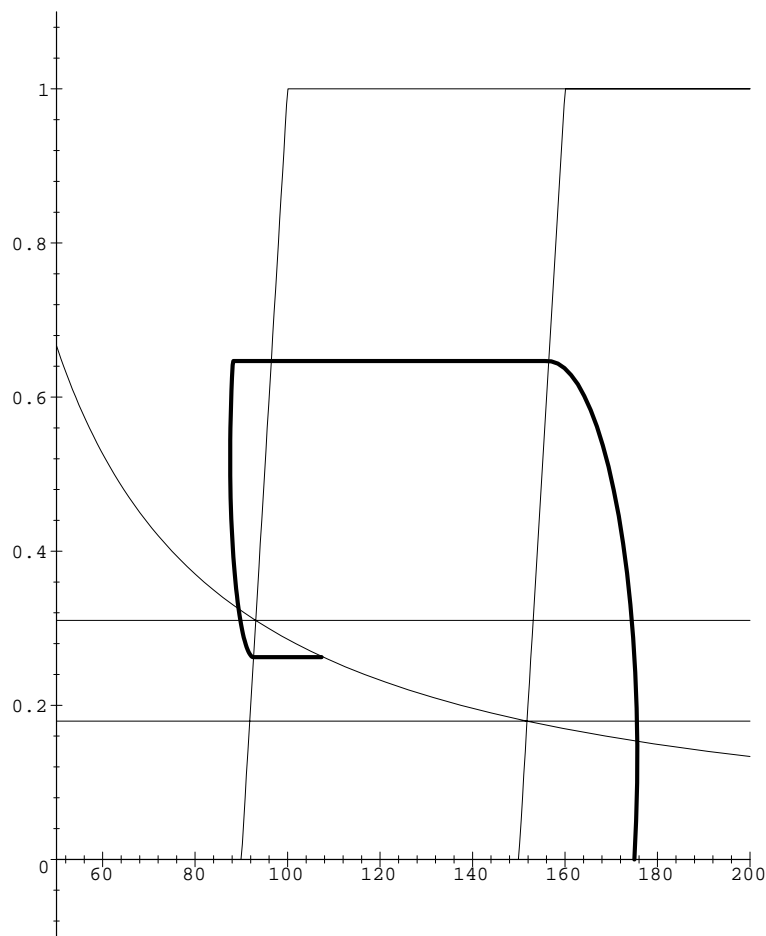
(a) $T_e - \omega$ plane.

Figure 13.

The geometric context of the following discussion is depicted in Figure 7, where the plane $\theta - \omega$ is shown together with the hysteresis curves and the graph of $g(y) = qh_r/(yh_r - q)$ which is found on the right-hand side in (3.8). As is suggested by Figures 5 and 6, the trajectories of the system in this plane and in parallel in the $T_e - \omega$ plane provide a way to visualize the effects of hysteresis on the system. The trajectory in the $\theta - \omega$ plane, given by $\{(\theta(t), \omega(t)) : 0 \leq t\}$, shows how θ is constrained to travel along the boundaries of the hysteresis region, or its horizontal segments. This movement is forced by (2.1) which defines the interaction between θ and T_e . And as θ evolves so does ω by (2.2). Simultaneously, the trajectory in the $T_e - \omega$ plane, given by $\{(T_e(t), \omega(t)) : 0 \leq t\}$, shows how T_e is constrained by the current setting of ω to move (horizontally) to the steady state described at the end of Section 4. And as T_e evolves, so does θ , again by (2.1). It is this interaction between the two subsystems (2.1),(2.2) and (2.3),(2.4), as illustrated in the $\theta - \omega$ and $T_e - \omega$ planes, that creates the dynamics of the whole system.

It is also instructive to consider the system trajectories in the $T_e - \omega$ plane, to follow the evolution of T_e more closely. For any give set $\{\omega_0, \theta_0, T_{e0}, T_{r0}\}$ of initial conditions, we wish to determine the trajectory of the pair $\{\theta(t), \omega(t)\}$ in the $\theta - \omega$ plane and the trajectory of $\{T_e(t), \omega(t)\}$ in the $T_e - \omega$ plane. Our main interest lies in the behavior of the solutions as $t \rightarrow \infty$.

We present four simulations which indicate that for appropriate choice of the initial conditions, the system parameters, and with different hysteresis curves, the system may approach each one of the continuum of steady solutions given in Section 3.2. These are represented in Figure 7 by



(b) $\theta - \omega$ plane, the full model.

Figure 13. (cont.)

the portion $C_L C_R$ of the curve g . Moreover, as was indicated above, by a very careful choice of the initial conditions, and by relaxing the requirement $\omega_0 = H_\beta(\theta_0)$, other points on the curve (below the horizontal line $\omega = 1$), can be approached asymptotically, and thus, act as steady states. To arrive at the opening ω^* which corresponds to a value of θ^* outside of the hysteresis region, we set $\omega_0 = \omega^*$, T_{0e} such that $\theta_0 < T_{0e} < \theta^*$. Then, as the system evolves, $\theta < T_e$ and as T_e approaches its steady state monotonically, the hysteresis keeps ω at its original and final value ω^* .

In all the simulations, we set $q = 25$, $h_r = 2$, the time steps were $\Delta t = 0.005$ and final time $T = 40$. Also, the initial conditions were chosen as $\theta_0 = 150$, $T_{e0} = 175$, $T_{r0} = 0.001$, and $\omega_0 = 0$. For each simulation we present the trajectory of the solution in the $T_e - \omega$ plane (a), and in the $T_e - \theta$ plane (b). Given the initial conditions, this means the trajectories originate at, or just beyond, the lower right corner of the hysteresis region and evolve counterclockwise. Almost all of them have been drawn using linear interpolation of 25% sample, equally spaced, of the full set of simulations results. Only in Figures 12a and 12b, we use the full set of results.

In Figure 8, we depict the simulation of the system with $h_e = 3$, which causes θ to follow T_e more closely, by (2.1). The hysteresis curves (shown in the figure) given by piecewise straight lines with $f_L = 0$ until $\theta = 90$, then a straight line with slope 0.1, and $f_L = 1$ for $100 \leq \theta$, and f_R with the same form, but translated 60 units to the right. The decay of the system, after about one and a half oscillations is seen clearly. The final approach seems to be rather slow.

In Figure 9, we show the system with hysteresis curves (shown) given by piecewise straight

lines with $f_L = 0$ until $\theta = 75$, then a straight line with slope 0.1, and $f_L = 1$ for $85 \leq \theta$, and f_R with the same form, but translated 75 units to the right. This lengthens the horizontal segments of the hysteresis region. Here we used $h_e = 1$. The decay of the system, after about one and a half oscillations is seen too.

In Figure 10, we depict the system with hysteresis curves (shown) given by $f_L = 0$ until $\theta = 90$, then a straight line with slope 0.0145, and $f_L = 1$ for $159 \leq \theta$, and f_R is zero up to $\theta = 150$, and then has the slope 0.1, and $f_R = 1$ for $160 \leq \theta$. This means that the thermostat opens more slowly than it closes. Also, $h_e = 1$. The system approaches the steady state in one cycle.

Finally in Figure 11, we have approach to the steady state without oscillations. Here, $f_L = 0$ until $\theta = 90$, then a straight line with slope 0.1, and $f_L = 1$ for $100 \leq \theta$, and f_R is zero up to $\theta = 150$, and then has the slope 0.01, and $f_R = 1$ for $250 \leq \theta$, with $h_e = 1$. Here, the thermostat opens faster than it closes.

These, and other numerical results we have obtained in the course of this investigation, give strong support to our conjecture at the end of Section 3.

Next, we present a rather surprising result, which shows that the model without delay can exhibit intrinsic oscillations too. The surprise is that in our previous papers it appeared that the system delay was an essential condition for such oscillations. Now, it seems that it is not so. In Figures 12a–12c, we depict the simulation with parameters $q = 25$, $h_r = 2.0$, $h_e = 1$, the time steps were $\Delta t = 0.005$ and final time $T = 40$, and hysteresis curves $f_L = 0$ until $\theta = 90$, then a straight line with slope 0.1, and $f_L = 1$ for $100 \leq \theta$, and f_R is zero up to $\theta = 150$, and then has the slope 0.1, and $f_R = 1$ for $100 \leq \theta$. It is seen that the system is capable of intrinsic oscillations.

We remark that all the examples above were obtained by changing only one of the parameters of this example (Figure 12). This indicates that the oscillations can be stabilized or controlled by changing only one value. This indicates that a more thorough investigation of these intrinsic oscillations is warranted, both numerically and analytically. It also explains our inability to prove that all solutions converge asymptotically to the steady solutions.

6.4. The Full Model

For the sake of completeness, we present one simulation of the full model, (2.1)–(2.6). We point out that more extensive simulations of the model can be found in [1], where the main interest was in the conditions for intrinsic oscillations. Additional simulations will be done in the near future.

The hysteresis was chosen as in Figure 8 above; $q = 25$, $h_r = 2$, $h_e = 1$, $V_e = V_r = 1$: the run was with 8000 time steps, each of $\Delta t = 0.005$; the delay was chosen as $\tau = 1.5$. In Figure 13 we depict the case where the initial conditions were as in Figure 12, where we found periodic oscillations.

We see that the introduction of a delay lead to the disappearance of the oscillations of Figure 12.

7. CONCLUSIONS

We described a model for the dynamic behavior of a thermostat-like device. The model was set as a system of three delay-differential equations for component temperatures and a functional relationship for the thermostat opening, which represents the hysteresis thermo-mechanical behavior of the valve. Our interest was in the steady states of the system and the approach of the solutions to the steady states.

In the case without hysteresis, i.e., when $\omega = f(\theta)$, we found that there exists a unique steady solution. When hysteresis is included, there may be a unique solution or there is a continuum of steady solutions. Based on our numerical simulations, we conjectured that each one of these can be reached by appropriate choice of (nonsteady) initial conditions. In addition, this system may have oscillatory solutions.

In the case when $\omega = \text{const.}$, we established the exponential decay of the solutions to the unique steady state. The theoretical consideration of the long term behavior of the solutions in the other cases remains open.

A computer algorithm, based on explicit time marching, has been employed to generate numerical solutions to simulate the model behavior. In Section 6.1, we depicted a typical simulation with $\omega = \text{const.}$ and its decay in time. In Section 6.2, we described two simulations without hysteresis, i.e., $\omega = f(\theta)$. Again, the convergence to the steady solution is clear.

In Section 6.3, we presented simulations of the system with hysteresis but without delay. The simulations indicate that each one of the continuum of steady solutions can be approached by proper choice of the system parameters. However, in some of the simulations we found that the system did not approach any steady solution, instead settled for intrinsic periodic oscillations. There exists a considerable interest in investigating the conditions for these oscillations, similarly to those in [1–3], both theoretically and numerically. This is motivated by the observation that, here, the intrinsic oscillations are induced without any delays. In contrast, delays were essential in the simpler models investigated in [2,3]. Therefore, we plan to continue our investigation of the model without delays and to try and establish conditions for the appearance of oscillatory solutions.

We conclude that the system which models thermostat-like devices can exhibit different types of behavior and there remain many interesting questions to be resolved.

APPENDIX

We present the model from [1] for the convenience of the reader.

THERMOSTAT MODEL. Find the functions $\{\theta, T_e, T_r, \omega\}$ such that

$$\frac{d}{dt}(c_*\theta + \lambda\omega) = h_{th}(T_e(t) - \theta(t)), \tag{A.1}$$

$$\omega(t) = H_\beta(\theta(t)), \tag{A.2}$$

$$(cV_e + c_{bl})\frac{dT_e}{dt} = q_e - c(v_r + v_h)(T_e(t) - T_{in}^e(t)), \tag{A.3}$$

$$T_{in}^e(t) = (v_r\omega(t)T_r(t - \tau_{ro}) + v_r(1 - \omega(t))T_e(t - \tau_r) + v_h(1 - \gamma)T_e(t - \tau_h) + v_h\gamma T_{ah})(v_r + v_h)^{-1}, \tag{A.4}$$

$$cV_r\frac{dT_r}{dt} = cv_r\omega(t)(T_e(t - \tau_{ri}) - T_r(t)) - h_r(T_r(t) - T_{amb}),$$

$$T_e(t) = T_{e0}(t), \quad T_r(t) = T_{r0}(t), \quad -\tau \leq t \leq 0, \\ \theta(0) = \theta_0, \quad \omega(0) = \omega_0.$$

Here, T_{e0}, T_{r0}, θ_0 and ω_0 are the initial conditions: T_{e0} and T_{r0} are given functions defined on the time interval $-\tau \leq t \leq 0$. This is due to the existence of the delays in the system. The initial condition for θ and ω is specified only at $t = 0$, since it is obtained from the known θ_0 via the hysteresis condition on the time interval $-\tau < t \leq 0$. Finally, the heat capacity c_* is given by

$$c_* = \begin{cases} c_{th}^s, & \text{if } \theta \leq T_L, \\ c_{th}^s + (c_{th}^l - c_{th}^s) \frac{\theta - T_L}{T_R - T_L}, & \text{if } T_L \leq \theta \leq T_R, \\ c_{th}^l, & \text{if } T_R \leq \theta, \end{cases}$$

where c_{th}^l and c_{th}^s are the heat capacities of the liquid and solid wax, respectively.

REFERENCES

1. X. Zou, J.A. Jordan and M. Shillor, A dynamic model for a thermostat, *J. Engng. Math.* **36**, 291–310, (1999).
2. B. Cahlon, D. Schmidt, M. Shillor and X. Zou, Analysis of thermostat models, *Euro. J. Appl. Math.* **8**, 437–455, (1997).
3. B. Cahlon, D. Schmidt, M. Shillor and X. Zou, Oscillations in thermostat models, *Adv. Math. Sci. Appl.* **9** (1), 25–49, (1999).
4. J.W. Macki, P. Nistri and P. Zecca, Mathematical models for hysteresis, *SIAM Review* **35** (1), 94–123, (1993).
5. A. Visintin, Mathematical models of hysteresis, In *Topics in Nonsmooth Mechanics*, (Edited by J.J. Moreau, P.D Panagiotopoulos and G. Strang), pp. 295–323, Birkhauser, Basel, (1988).
6. S.P. Tomlinson and C.R. Burrows, Design of a feedback controlled thermostat for a vehicle cooling system, SAE Intl. Off Highway and Powerplant Congress and Exp., August 26–28, 1996, Indianapolis, IN.